



1 **Measurements of higher alkanes using NO⁺ PTR-ToF-**
2 **MS: significant contributions of higher alkanes to**
3 **secondary organic aerosols in China**

4 Chaomin Wang^{1,2}, Caihong Wu^{1,2}, Sihang Wang^{1,2}, Jipeng Qi^{1,2}, Baolin Wang³, Zelong
5 Wang^{1,2}, Weiwei Hu⁴, Wei Chen⁴, Chenshuo Ye⁵, Wenjie Wang⁵, Yele Sun⁶, Chen Wang³,
6 Shan Huang^{1,2}, Wei Song⁴, Xinming Wang⁴, Suxia Yang^{1,2}, Shenyang Zhang^{1,2}, Wanyun
7 Xu⁷, Nan Ma^{1,2}, Zhanyi Zhang^{1,2}, Bin Jiang^{1,2}, Hang Su⁸, Yafang Cheng⁸, Xuemei Wang^{1,2},
8 Min Shao^{1,2,*}, Bin Yuan^{1,2,*}

9 ¹ Institute for Environmental and Climate Research, Jinan University, 511443 Guangzhou, China

10 ² Guangdong-Hongkong-Macau Joint Laboratory of Collaborative Innovation for Environmental Quality,
11 511443 Guangzhou, China

12 ³ School of Environmental Science and Engineering, Qilu University of Technology, 250353 Jinan, China

13 ⁴ State Key Laboratory of Organic Geochemistry and Guangdong Key Laboratory of Environmental
14 Protection and Resources Utilization, Guangzhou Institute of Geochemistry, Chinese Academy of Sciences,
15 510640 Guangzhou, China

16 ⁵ State Joint Key Laboratory of Environmental Simulation and Pollution Control, College of Environmental
17 Sciences and Engineering, Peking University, 100871 Beijing, China

18 ⁶ State Key Laboratory of Atmospheric Boundary Physics and Atmospheric Chemistry, Institute of
19 Atmospheric Physics, Chinese Academy of Sciences, 100029 Beijing, China

20 ⁷ State Key Laboratory of Severe Weather & Key Laboratory for Atmospheric Chemistry of China
21 Meteorology Administration, Chinese Academy of Meteorological Sciences, 100081 Beijing, China

22 ⁸ Multiphase Chemistry Department, Max Planck Institute for Chemistry, Mainz 55128, Germany

23 *Email: Bin Yuan (byuan@jnu.edu.cn) and Min Shao (mshao@pku.edu.cn)

24 **Abstract:** Higher alkanes are a major class of intermediate-volatility organic compounds
25 (IVOCs), which have been proposed to be important precursors of secondary organic



26 aerosols (SOA) in the atmosphere. Accurate estimation of SOA from higher alkanes and
27 their oxidation processes in the atmosphere are limited, partially due to difficulty in their
28 measurements. High-time resolution (10 s) measurements of higher alkanes were performed
29 using a novel online mass spectrometry method at an urban site of Guangzhou in Pearl River
30 Delta (PRD) and at a rural site in North China Plain (NCP), respectively. High concentrations
31 were observed in both environments, with significant diurnal variations. At both sites, SOA
32 production from higher alkanes is estimated from their photochemical losses and SOA yields.
33 Higher alkanes account for significant fractions of SOA formation at the two sites, with
34 average contributions of $7.0\pm 8.0\%$ in Guangzhou and $7.1\pm 9.5\%$ in NCP, which are
35 comparable or even higher than both single-ring aromatics and naphthalenes. The significant
36 contributions of higher alkanes in SOA formation suggests that they should be explicitly
37 included in current models for SOA formation. Our work also highlights the importance of
38 NO^+ PTR-ToF-MS in measuring higher alkanes and quantifying their contributions to SOA
39 formation.

40



41 **1. Introduction**

42 As important components of fine particles, secondary organic aerosols (SOA) not
43 only affect air quality and climate change, but also threaten human health (An et al.,
44 2019;Zhu et al., 2017;Chowdhury et al., 2018). Recent studies indicate large discrepancies
45 between simulations and observations for SOA (de Gouw et al., 2008;Dzepina et al.,
46 2009;Jiang et al., 2012), which are attributed to limited understanding of complicated
47 chemical and physical processes underlying SOA formation (Hallquist et al., 2009). A
48 volatility basis set (VBS) model was developed to advance SOA modeling by lumping
49 numerous, yet unidentified, precursors based on their volatility (Donahue et al., 2006), which
50 substantially improved the agreement between SOA simulations and observations (Hodzic
51 et al., 2010). However, there are still large uncertainties in current VBS models, including
52 rate constants of oxidation reactions, the change of O/C ratio in oxidation, and the relative
53 importance of functionalization and fragmentation (Ma et al., 2017;Hayes et al., 2015).
54 Explicit consideration of individual or a group of important semi-volatile or intermediate
55 volatile organic compounds (S/I-VOCs) in the SOA model are urgently needed.

56 Higher alkanes as a major class of IVOCs (roughly corresponding to alkanes with
57 12-20 carbons) have been proposed as important SOA contributors in urban areas (Robinson
58 et al., 2007;Yuan et al., 2013;Zhao et al., 2014a). Higher alkanes are estimated to produce as
59 much as or even more SOA than single-ring aromatics and polycyclic aromatic hydrocarbons
60 from the oxidation of vehicle emissions, based on the chemical compositions measurements
61 of vehicle exhausts (Tkacik et al., 2012b;Zhao et al., 2016a). Previous model studies
62 suggested that SOA simulation can be significantly improved when higher alkanes were
63 considered in the model (Pye and Pouliot, 2012;Jathar et al., 2014). Although the
64 concentrations of higher alkanes might be lower than other VOCs classes (e.g. aromatics) in



65 the atmosphere, higher alkanes are found to have much higher SOA yields and the yields
66 increase steadily with carbon number (Lim and Ziemann, 2005;Lim and Ziemann,
67 2009;Presto et al., 2010a). For a given carbon number, SOA yields of higher alkanes reduce
68 with branching of the carbon chain, especially under high-NO_x conditions (Lim and Ziemann,
69 2009;Tkacik et al., 2012a;Loza et al., 2014).

70 Higher alkanes, predominantly *n*-alkanes, have been mainly measured by gas
71 chromatography-based techniques, focusing on the compositions (Gong et al., 2011;Caumo
72 et al., 2018), atmospheric concentration levels (Bi et al., 2003;Anh, 2018) and gas-particle
73 partitioning (Xie et al., 2014;Sangiorgi et al., 2014). While most of previous studies collected
74 offline samples (usually 0.5 day-1 week) for GC-based analysis in the laboratory, hourly
75 online measurements of *n*-alkanes using GC-based thermal desorption aerosol gas
76 chromatograph for semi-volatile organic compounds (SV-TAG) was recently developed and
77 applied in ambient air (Zhao et al., 2013). Proton-transfer-reaction mass spectrometry (PTR-
78 MS) using H₃O⁺ as reagent ions are capable of measurements for many organic compounds
79 with high time response and sensitivity (de Gouw and Warneke, 2007;Jordan et al.,
80 2009;Yuan et al., 2017b). Although H₃O⁺ PTR-MS is response to large alkanes (>C₈), these
81 alkanes usually fragment into small masses with mass spectra difficult to interpret (Jobson
82 et al., 2005;Gueneron et al., 2015). Recently, PTR-MS using NO⁺ as reagent ions was
83 demonstrated to provide fast online measurement of higher alkanes (Erickson et al.,
84 2014;Koss et al., 2016;Inomata et al., 2013). The high-time resolution measurements of
85 higher alkanes provide valuable information for SOA estimation, as the dependence of SOA
86 yields on organic aerosol concentrations and other environmental parameters (e.g.
87 temperature) (Lim and Ziemann, 2009;Presto et al., 2010a;Loza et al., 2014;Lamkaddam et
88 al., 2017a) can be taken into account in more details.



89 In this study, we utilize NO^+ PTR-ToF-MS to measure higher alkanes at two different
90 sites in China, one urban site in Pearl River Delta region and one rural site in North China
91 Plain region. We use the datasets along with measurements of other pollutants to estimate
92 contributions to SOA formation from higher alkanes and other SOA precursors. The
93 observation-constrained SOA formation of this study is a step forward upon previous
94 modelling studies, which proposed the important roles of S/I-VOCs (Jiang et al., 2012; Yang
95 et al., 2018; Wu et al., 2019) including higher alkanes (Yuan et al., 2013) in SOA formation
96 in China.

97 **2. Methods**

98 Field campaigns were conducted at an urban site of Guangzhou in the Pearl River
99 Delta (PRD) region during September-November 2018 and at a rural site of Baoding in North
100 China Plain (NCP) during November-December 2018, respectively. The detailed description
101 of the measurement sites can be found in Supporting Information (SI, Figure S1).

102 **2.1 NO^+ PTR-ToF-MS measurements**

103 Proton-transfer-reaction mass spectrometry (PTR-MS) is a technique that allows for
104 fast and sensitive measurements of volatile organic compounds (VOCs) at trace levels in air.
105 PTR-MS using H_3O^+ chemistry makes possible of quantitative of alkenes, aromatics, and even
106 oxygenated VOCs (Yuan et al., 2017a). Here, PTR-MS with NO^+ chemistry was used to detect
107 higher alkanes, through hydride abstraction by NO^+ forming mass ($m-1$) ions (m is the
108 molecular mass) (Erickson et al., 2014; Koss et al., 2016; Inomata et al., 2013).

109 A commercially available PTR-ToF-MS instrument (Ionicon Analytik, Austria) with
110 a mass resolution of 5500 $m/\Delta m$ was used for this work. To generate NO^+ as reagent ions,
111 ultra-high-purity air (5.0 sccm) was directed into the hollow cathode discharge ion sources.



112 The pressure of the drift tube was maintained at 3.8 mbar. Voltages of ion source and drift
113 chamber were explored (Figure S2) to optimize the generation of NO^+ ions relative to H_3O^+ ,
114 O_2^+ , and NO_2^+ and minimize alkane fragmentation. Ion source voltages of U_s and U_{so} were
115 selected as 40 V and 120 V, while U_{drift} and U_{dx} were set to 470 V and 23.5 V, resulting in
116 an E/N (electric potential intensity relative to gas number density of 60 Td. NO^+ PTR-ToF-
117 MS data was analysed using Tofware software (Tofwerk AG) for high-resolution peak-fitting.
118 A description of the algorithm can be found in Stark et al. (2015) and Timonen et al. (2016).
119 Figure 1 shows the high-resolution peak fitting to the averaged mass spectra on a typical day
120 (12 October 2018) for m/z 169, m/z 211 and m/z 281, at which masses produced by dodecane
121 ($\text{C}_{12}\text{H}_{25}^+$), pentadecane ($\text{C}_{15}\text{H}_{31}^+$) and eicosane ($\text{C}_{20}\text{H}_{41}^+$) are detected. It is observed that the
122 ions from higher alkanes lie at the right-most position at each nominal mass, with signals
123 either the largest or among the largest ions at these nominal masses, which help to achieve
124 high precision for determined signals of higher alkanes from high-resolution peak fitting
125 (Cubison and Jimenez, 2015; C. Corbin et al., 2015).

126 In this study, we normalize the raw ion count rate of higher alkanes to the primary ion
127 (NO^+) at a level of 10^6 cps to account for fluctuations of ion source and detector. Calibrations
128 were conducted every 1-2 days under both dry conditions ($\text{RH} < 1\%$) and ambient humidity
129 conditions using a gas standard with a series of *n*-alkanes (Apel Riemer Environmental Inc.)
130 during both two field campaigns (Figure 2(a)). Calibration factors of *n*-alkanes (C8-C15)
131 standards were stable during the campaigns (Figure S3). Humidity-dependent behaviours of
132 these *n*-alkanes (C8-C15) were performed in the laboratory under different humidity by
133 diluting higher alkanes standard into humidified air to reach approximately 1 ppb mixing ratio.
134 As shown in Figure 2(b, c), like *n*-dodecane and *n*-pentadecane, the normalized signal of all
135 higher alkanes decreased slightly with increasing humidity. The humidity effects on higher
136 alkanes for both campaigns were corrected using the laboratory established relationships.



137 The fragmentation patterns for selected *n*-alkanes and their branched isomers are
138 measured with NO⁺ PTR-ToF-MS by introducing commercially acquired pure chemicals
139 (Figure S4). Figure 3(a) shows the fractions of hydride abstraction m-1 ions in the mass
140 spectra of C8-C20 *n*-alkanes in NO⁺ PTR-ToF-MS. Generally, larger *n*-alkanes show less
141 degree of fragmentation in the mass spectra with higher fractions contributed by m-1 ions.
142 The fraction of m-1 ions account for more than 60% of total ion signals for >C12 *n*-alkanes.
143 We also observe good correlation between the fractions of m-1 ions in mass spectra and the
144 determined sensitivities for C8-C15 *n*-alkanes. As C16-C21 *n*-alkanes exhibit similar degrees
145 of fragmentation as C15, sensitivities of the alkanes were assumed to be same as that of C15
146 *n*-alkane (Figure 3(b)). Comparison of the degree of fragmentation between *n*-alkanes and
147 their branched isomers (Figure S5) show the substituted group affect little on the degrees of
148 fragmentation for product ions, at least for branched isomers with up to 4 substituted methyl
149 groups. Previous studies demonstrated that the branched alkanes from emissions of fossil fuel-
150 related sources are primarily with one or two alkyl branches (Chan et al., 2013; Isaacman et
151 al., 2012). Therefore, we conclude that the branched isomers of higher alkanes should have
152 similar response factors to their normal analogues. As a result, the concentration of higher
153 alkanes by NO⁺ PTR-ToF-MS should be regarded as the summed concentrations of *n*-alkanes
154 and branched alkanes that have the same chemical formulas.

155 Detection limits are calculated as the concentrations at which signal counts are 3 times
156 of standard deviation of measured background counts (Bertram et al., 2011; Yuan et al., 2017b).
157 As shown in Table 1, detection limits are determined to be on the order of 0.7-1.3 ppt for
158 higher alkanes for 1 min integration times. Response time is calculated as the time required
159 to observe a 1/e²-signal decay after quick removal of the analyte from the sampled air
160 (Mikoviny et al., 2010). Response times for various alkanes are better than 1 min, except for
161 C21 alkanes (116 s) (Table1).



162 During these two campaigns, PTR-ToF-MS automatically switches between H_3O^+ and
163 NO^+ chemistry every 10-20 minutes with a 10 s resolution of measurement. Ambient air was
164 continuously introduced into PTR-ToF-MS through a Teflon tubing with an external pump at
165 5.0 L/min. The calculated residence time in Teflon tubing is ~ 7.6 s for PRD campaign and
166 ~ 3.0 s for NCP campaign, respectively. PTR-ToF-MS instrument was operating in a room
167 with a constant temperature of 20 °C. An insulating tube with stable temperature of 40 °C was
168 used to wrap outside of the sampling tubing to avoid water vapor condensation. Background
169 measurement of 3 minutes was conducted in each cycle of NO^+ and H_3O^+ measurements by
170 introducing the ambient air into a catalytic converter with a constant temperature of 367 °C.

171 **2.2 Other measurements**

172 During the Guangzhou campaign, an online GC-MS/FID system was used to measure
173 C2-C11 alkanes, alkenes and aromatics with a time resolution of one hour (Yuan et al., 2012).
174 Non-refractory components in particulate matter with diameter less than 1 μm (PM_{10})
175 including nitrate, sulfate, ammonium, chloride, and organics were measured with an
176 Aerodyne high-resolution time-of-flight aerosol mass spectrometric (HR-ToF-AMS) and a
177 time-of-flight aerosol chemical speciation monitor (ToF-ACSM) in PRD and NCP,
178 respectively. Trace gaseous species (CO , NO , NO_2 , O_3 , and SO_2) were measured using
179 commercial gas analyzers (Thermo Scientific). Photolysis frequencies were measured using
180 a spectroradiometer (PFS-100, Focused Photonics Inc.). In addition, temperature, pressure,
181 relative humidity and wind were continuously measured during two campaigns.

182 **3. Results and Discussion**

183 **3.1 Ambient concentrations and diurnal variations of higher alkanes**



184 Although NO^+ chemistry has been shown to be valuable in measuring many organic
185 species, the applications in real atmosphere of different environments are still limited (Koss et
186 al., 2016). Here, we compared the measurements of various VOCs from NO^+ PTR-ToF-MS
187 with both H_3O^+ PTR-ToF-MS and GC-MS/FID during the two campaigns. Overall, good
188 agreements between PTR-ToF-MS (both H_3O^+ and NO^+ chemistry) and GC-MS/FID are
189 obtained for aromatics (Figure S6). Consistent results of oxygenated VOCs are also obtained
190 between H_3O^+ and NO^+ chemistry (Figure S7). The time series and diurnal variations of
191 alkanes (C8-C11) between NO^+ PTR-ToF-MS and GC-MS/FID are shown in Figure 4 (and
192 Figure S8). Similar temporal trends for these alkanes are observed from the two instruments.
193 However, the concentrations at each carbon number from NO^+ PTR-ToF-MS are ~3-6 times
194 those from GC-MS/FID. This is expected, as dozens to hundreds of isomers exist for alkanes
195 with carbon number at this range (Goldstein and Galbally, 2007) and GC-MS/FID only
196 measured one or a few isomers. Based on measurements from NO^+ PTR-ToF-MS and GC-
197 MS/FID, we compute the molar concentration fractions of *n*-alkanes for each carbon number
198 (Figure 5). We found the fractions are in the range of 11%-21% for carbon number of 8-11,
199 which are comparable with results of ambient air in California, vehicle exhausts and diesel
200 fuel (Figure 5) (Chan et al., 2013; Gentner et al., 2012; Isaacman et al., 2012). These results
201 indicate the importance of branched alkanes in concentrations of higher alkanes and their
202 potential contributions to SOA formation. It also has strong implication for the merits of NO^+
203 PTR-ToF-MS in measuring sum of the alkanes with the same formula for estimation of SOA
204 contributions, as discussed later.

205 Table 2 summarizes means and standard deviations of concentrations of C8-C21
206 higher alkanes measured in PRD and in NCP, respectively. The mean concentrations of *n*-
207 alkanes measured at a suburban site in Paris (Ait-Helal et al., 2014) and an urban site in
208 Pasadena, U.S. (Zhao et al., 2014a) are also included in Table 1 for comparison. According



209 to the fraction of *n*-alkanes, the mean concentrations of *n*-alkanes in China are found to be
210 comparable to that from Paris and higher than in Pasadena. In general, concentrations of
211 higher alkanes concentration decrease with the increase of carbon number, with octanes (C8)
212 at ~0.5 ppb and heneicosanes (C21) at ~0.002 ppb. This decrease pattern of carbon distribution
213 are as the results of lower emissions from sources (Gentner et al., 2012), larger reactivity
214 towards OH radicals (Atkinson et al., 2008;Keyte et al., 2013) and larger fractions partitioning
215 to particles (Liang et al., 1997;Xie et al., 2014;Zhao et al., 2013) in the atmosphere.

216 The diurnal variations of selected higher alkanes are shown in Figure 6. C12 alkanes
217 and C15 alkanes exhibit similarly strong diurnal variations at both sites, with a relatively
218 high levels at night and minimum concentrations detected in the late afternoon at both sites.
219 Such diurnal variations are consistent with other primary VOCs species (e.g. aromatics), as
220 the result of both shallow boundary layer heights at night and faster chemical removal in the
221 daytime. The diurnal profiles of other higher alkanes are similar to C12 and C15 alkanes.

222 **3.2 Estimation of the contributions of higher alkanes to SOA formation**

223 A time-resolved approach based on consideration of photooxidation processes with
224 OH radical (Ait-Helal et al., 2014) was applied to estimate contributions of higher alkanes
225 to SOA during these two campaigns. In order to evaluate the relative importance to SOA
226 from different precursors, the same method was also used for monoaromatics, naphthalenes,
227 and isoprenoids.

228 This method considers the amount of chemical removal based on the parameterized
229 photochemical age, which was widely used to quantify contributions of different VOC
230 precursors to SOA formation (Zhao et al., 2014a;Ait-Helal et al., 2014;de Gouw et al., 2009).
231 The contributions to SOA formation from different compounds are determined by the ratios
232 of calculated SOA production amounts from individual precursors and SOA concentrations



233 derived from factor analysis of OA measurements by AMS (SI, Appendix 3). In this method,
234 SOA formation for a given compound can be estimated by

$$235 \quad [SOA_i]_t = [VOC_i]_t \times (e^{k_{VOC_i} \times ([OH] \times \Delta t)} - 1) \times Yield_i \quad (1)$$

236 where $[SOA_i]_t$ is the calculated SOA production ($\mu\text{g m}^{-3}$) for a given specific compound VOC_i
237 at time t , $[VOC_i]_t$ is the VOC_i concentration measured at time t ($\mu\text{g m}^{-3}$), $Yield_i$ is the SOA
238 yield data summarized from chamber studies, k_{VOC_i} is the rate constant of VOC_i with the OH
239 radical ($\text{cm}^3 \text{ molecule}^{-1} \text{ s}^{-1}$). The OH exposure, $[OH] \times \Delta t$ ($\text{molecules cm}^{-3} \text{ s}$), is estimated by
240 the ratio m+p-xylene and ethylbenzene with different reactivity for anthropogenic VOCs and
241 by the oxidation processes of isoprene for biogenic VOCs, respectively (Apel et al., 2002) (see
242 details in Figure S9). Since biogenic emissions were pretty weak during cold winter (mean
243 temperature 0.5 ± 3.6 °C) during NCP campaign, measured concentrations of isoprene and
244 monoterpenes are attributed to be of anthropogenic origin during the winter campaign in NCP
245 campaign, especially given the fact that they showed similar variations, diurnal profiles and
246 strong correlation with CO and anthropogenic VOCs species (Figure S10). A previous study
247 in Helsinki also found the importance of anthropogenic emission in monoterpene
248 concentrations (Hellén et al., 2012).

249 Based on equation (1), SOA production from higher alkanes (C8-C21 alkanes),
250 monoaromatics (benzene, toluene, C8 aromatics, C9 aromatics, styrene), naphthalenes
251 (naphthalene, methylnaphthalenes, dimethylnaphthalenes) and isoprenoids (isoprene,
252 monoterpenes) were calculated. The OH reaction rate constant of each compound was taken
253 from literature (Atkinson, 2003). SOA yield data used here for higher alkanes (Lim and
254 Ziemann, 2009; Presto et al., 2010b; Loza et al., 2014; Lamkaddam et al., 2017b),
255 monoaromatics (Li et al., 2016; Ng et al., 2007; Tajuelo et al., 2019), naphthalenes (Chan et al.,
256 2009) and isoprenoids (Ahlberg et al., 2017; Carlton et al., 2009; Edney et al., 2005; Kleindienst



257 et al., 2006; Pandis et al., 1991) were summarized from reported values in the literature, with
258 the consideration of the influence of organic aerosol concentration (Figure S11) to SOA yields
259 (Donahue et al., 2006) (Figure S12-13).

260 Both OH reaction rate constants and SOA yields of *n*-alkanes reported in the literature
261 are applied for higher alkanes, as most of the chamber studies have focused on *n*-alkanes. The
262 OH reaction rate constants of branched alkanes are higher than those of *n*-alkanes, while their
263 SOA yields are lower than *n*-alkanes, of which both depending on chemical structures of the
264 carbon backbone (Lim and Ziemann, 2009; Tkacik et al., 2012a; Loza et al., 2014). The
265 combined effects are hard to evaluate due to limited data, but the two effects can partially (if
266 not all) cancel out. As shown above, temperature (mean temperature 0.5 ± 3.6 °C) in NCP
267 winter campaign was significantly lower than the temperature (usually 25 °C) at which SOA
268 yields are derived from chamber studies. Temperature can significantly influence SOA yields,
269 with higher yields at lower temperature (Takekawa et al., 2003; Lamkaddam et al., 2017b). It
270 might cause underestimation of SOA production from various precursors in winter of NCP.

271 The calculated results of SOA production for different higher alkanes are shown in
272 Figure 7. Although lower concentrations of heavier alkanes were observed for both
273 campaigns, the calculated SOA production are largest for C12-C18 (Figure 7(b)). This is
274 because of two reasons: (1) Alkanes with larger carbon number have larger SOA yields. The
275 calculated SOA yields using the average OA concentrations during the two campaigns are
276 both larger than 0.2 for >C12 alkanes and increase to near unity for C20-C21 alkanes. (2)
277 Larger alkanes are relatively more reactive than lighter ones, which results in larger
278 proportions of calculated concentrations that have been chemically consumed in the
279 atmosphere. It is interesting to note that the distribution of contributions from alkanes with
280 different carbon number to SOA formation shown here is in good agreement with the
281 previous results referred from volatility calculation for precursors (de Gouw et al.,



282 2011;Liggio et al., 2016). The magnitudes of photochemical processes are apparently
283 different between the two campaigns, with larger calculated OH exposure in the PRD
284 campaign in autumn than the NCP campaign in winter (Figure S9). Consequently, the
285 calculated chemical losses of alkane concentrations and their SOA production are much
286 higher in PRD, though measured alkane concentrations are comparable during the two
287 campaigns.

288 Along with higher alkanes, SOA production for monoaromatics, naphthalenes and
289 isoprenoids are shown in Figure 8 (and Figure S14-16). The total average SOA production
290 from C8-C21 alkanes are $0.6\pm 0.8 \mu\text{g m}^{-3}$ and $1.1\pm 1.2 \mu\text{g m}^{-3}$ in PRD and NCP, respectively.
291 The formed SOA from higher alkanes account for $7.0\pm 8.0\%$ and $7.1\pm 9.5\%$ of SOA formation
292 in PRD and NCP, respectively. The contributions of monoaromatics to SOA formation are
293 $6.2\pm 7.7\%$ and $9.4\pm 17.4\%$ in PRD and NCP, respectively. Naphthalenes have been proposed
294 to be important precursors of SOA from laboratory chamber studies (Kleindienst et al., 2012).
295 In this study, we determine $2.8\pm 4.6\%$ of SOA in PRD and $11.1\pm 14.3\%$ of SOA in NCP are
296 contributed by naphthalenes. The SOA contribution from naphthalenes determined for NCP
297 is comparable to the results ($10.2\pm 1.0\%$) obtained during haze events in Beijing in a recent
298 study (Huang et al., 2019). Significant contribution from monoterpenes to SOA ($8.7\pm 14.6\%$)
299 is observed in NCP. As mentioned above, we attribute these isoprene and monoterpenes to
300 anthropogenic emissions, including vehicle exhausts and biomass combustions in this region.
301 The SOA precursors considered in this study in total could explain 14.9%-29.0% and 18.1-
302 119.9% of SOA formation in PRD and NCP, respectively. The lower explained percentages
303 of SOA formation during the highly polluted periods and during the daytime in NCP (Figure
304 S14(b)) imply that some other SOA precursors or formation pathways (e.g. aqueous reactions)
305 are contributing significantly to SOA formation of the strong haze pollution in NCP.
306 Compared to a previous study in northern China (Yuan et al., 2013), the missing gap of SOA



307 formation declined after explicitly considering higher alkanes and naphthalenes in SOA
308 production.

309 As shown in Figure 8, we find that C8-C21 higher alkanes contribute significantly to
310 SOA formation at both an urban site in autumn of PRD and a rural site in winter of NCP.
311 The contributions from higher alkanes are either comparable or higher than both
312 monoaromatics and naphthalenes. An independent estimation method by considering SOA
313 instantaneous production rates obtained similar results (Figure S18), which confirms the
314 results from the photochemical age based on parameterization method shown above. The
315 importance of higher alkanes in SOA formation has been also proposed in several previous
316 SOA modelling studies (Pye and Pouliot, 2012; Zhao et al., 2014b). These results, along with
317 our results from observations in ambient atmosphere, underline that the inclusion of higher
318 alkanes in SOA models in the atmosphere should be considered if possible.

319 **4. Conclusions**

320 In this study, we utilized a NO^+ PTR-TOF-MS to measure C8-C21 alkanes in two
321 different environments in China. Based on a series of laboratory experiments, we show that
322 NO^+ PTR-TOF-MS can provide online measurements of higher alkanes with high accuracy
323 and fast response. The measured concentrations of higher alkanes were relatively high during
324 the two campaigns. The diurnal profiles of higher alkanes are similar to anthropogenic VOCs,
325 implying they are emitted from anthropogenic sources.

326 On the basis of measurements of higher alkanes by NO^+ PTR-TOF-MS, we successfully
327 take into account their contributions in SOA formation. The time-resolved measurements of
328 higher alkanes by NO^+ PTR-ToF-MS provide the opportunity to accurately apply the
329 photochemical age-based parametrization method. As there is no separation before detection
330 in PTR-ToF-MS, the measured concentrations of NO^+ PTR-ToF-MS represent all of the



331 compounds that contribute to the product ions ($m-1$ ions), which include concentrations from
332 both n -alkanes and branched alkanes. With the total concentration of both n -alkanes and
333 branched alkanes quantified, the contribution from higher alkanes at each carbon number can
334 be estimated as a whole. This is an important supplementary method to the traditional
335 analytical method by GC techniques for higher alkanes, as fully chemical separation and
336 detection of numerous isomers of higher alkanes remain as a challenge, even using the most
337 advanced GC \times GC-ToF-MS instruments (Chan et al., 2013; Alam et al., 2016).

338 Higher alkanes were found to have significant contributions to SOA in both PRD and
339 NCP regions with a similar or even higher contributions than that of monoaromatics and
340 naphthalenes. The importance of higher alkanes to SOA formation also call for more work
341 to investigate emissions and chemistry of these compounds in the atmosphere. It was shown
342 that fossil-related combustions such as vehicle exhausts are major sources for higher alkanes
343 (Zhao et al., 2016b). While, recent studies pointed out the potential large influence of non-
344 combustion sources, e.g., solvent use, on emissions of higher alkanes (McDonald et al.,
345 2018; Khare and Gentner, 2018). However, such quantitative information on emissions of
346 higher alkanes is still limited. The measurements of higher alkanes by NO^+ PTR-ToF-MS
347 with fast response could help to fill these research gaps.

348



349 **Acknowledgements**

350 This work was supported by the National Key R&D Plan of China (grant No.
351 2018YFC0213904, 2016YFC0202206), the National Natural Science Foundation of China
352 (grant No. 41877302), Guangdong Natural Science Funds for Distinguished Young Scholar
353 (grant No. 2018B030306037), Guangdong Provincial Key R&D Plan (grant No.
354 2019B110206001), Guangdong Soft Science Research Program (grant No.
355 2019B101001005) and Guangdong Innovative and Entrepreneurial Research Team Program
356 (grant No. 2016ZT06N263). Weiwei Hu and Wei Chen were supported by National Natural
357 Science Foundation of China (grant No. 41875156). The authors gratefully acknowledge the
358 science team for their technical support and discussions during the campaigns in PRD and
359 NCP.

360 **Data availability**

361 Data is available from the authors upon request

362 **Competing interests**

363 The authors declare that they have no conflicts of interest

364 **Author contributions**

365 BY and MS designed the research. CMW, CHW, SHW, JPQ, BLW, WC, CW, WS and
366 WYX contributed to data collection. CMW performed the data analysis, with contributions
367 from ZLW, WWH and CSY. CMW and BY prepared the manuscript with contributions from
368 other authors. All the authors reviewed the manuscript.



369 References

- 370 Ahlberg, E., Falk, J., Eriksson, A., Holst, T., Brune, W. H., Kristensson, A., Roldin, P., and
371 Svenningsson, B.: Secondary organic aerosol from VOC mixtures in an oxidation flow reactor,
372 *Atmospheric Environment*, 161, 210-220, 10.1016/j.atmosenv.2017.05.005, 2017.
- 373 Ait-Helal, W., Borbon, A., Sauvage, S., de Gouw, J. A., Colomb, A., Gros, V., Freutel, F., Crippa, M.,
374 Afif, C., Baltensperger, U., Beekmann, M., Doussin, J. F., Durand-Jolibois, R., Fronval, I., Grand, N.,
375 Leonaridis, T., Lopez, M., Michoud, V., Miet, K., Perrier, S., Prevot, A. S. H., Schneider, J., Siour, G.,
376 Zapf, P., and Locoge, N.: Volatile and intermediate volatility organic compounds in suburban Paris:
377 variability, origin and importance for SOA formation, *Atmospheric Chemistry and Physics*, 14, 10439-
378 10464, 10.5194/acp-14-10439-2014, 2014.
- 379 Alam, M. S., Stark, C., and Harrison, R. M.: Using Variable Ionization Energy Time-of-Flight Mass
380 Spectrometry with Comprehensive GCxGC To Identify Isomeric Species, *Analytical Chemistry*, 88,
381 4211-4220, 10.1021/acs.analchem.5b03122, 2016.
- 382 An, Z., Huang, R. J., Zhang, R., Tie, X., Li, G., Cao, J., Zhou, W., Shi, Z., Han, Y., Gu, Z., and Ji, Y.:
383 Severe haze in northern China: A synergy of anthropogenic emissions and atmospheric processes, *Proc*
384 *Natl Acad Sci U S A*, 116, 8657-8666, 10.1073/pnas.1900125116, 2019.
- 385 Anh, H. Q. T., K., Tue, N. M.; Tuyen, L. H.; Chi, N. K.; Minh, T. B.; Viet, P. H.; Takahashi, S. : A
386 preliminary investigation of 942 organic micro-pollutants in the atmosphere in waste processing and
387 urban areas, northern Vietnam: Levels, potential sources, and risk assessment, *Ecotoxicol. Environ. Saf.*,
388 167, 354-364, 2018.
- 389 Apel, E. C., Riemer, D. D., Hills, A., Baugh, W., Orlando, J., Faloon, I., Tan, D., Brune, W., Lamb,
390 B., Westberg, H., Carroll, M. A., Thornberry, T., and Geron, C. D.: Measurement and interpretation of
391 isoprene fluxes and isoprene, methacrolein, and methyl vinyl ketone mixing ratios at the PROPHET
392 site during the 1998 Intensive, *Journal of Geophysical Research: Atmospheres*, 107, ACH 7-1-ACH 7-
393 15, 10.1029/2000JD000225, 2002.
- 394 Atkinson, R.: Kinetics of the gas-phase reactions of OH radicals with alkanes and cycloalkanes,
395 *Atmospheric Chemistry and Physics*, 3, 2233-2307, 10.5194/acp-3-2233-2003, 2003.
- 396 Atkinson, R., Arey, J., and Aschmann, S. M.: Atmospheric chemistry of alkanes: Review and recent
397 developments, *Atmospheric Environment*, 42, 5859-5871, 10.1016/j.atmosenv.2007.08.040, 2008.
- 398 Bertram, T., Kimmel, J., Crisp, T., Ryder, O., Yatavelli, R., Thornton, J., Cubison, M., Gonin, M., and
399 Worsnop, D.: A field-deployable, chemical ionization time-of-flight mass spectrometer, *Atmospheric*
400 *Measurement Techniques*, 4, 1471-1479, 10.5194/amt-4-1471-2011, 2011.
- 401 Bi, X. H., Sheng, G. Y., Peng, P., Chen, Y. J., Zhang, Z. Q., and Fu, J. M.: Distribution of particulate-
402 and vapor-phase n-alkanes and polycyclic aromatic hydrocarbons in urban atmosphere of Guangzhou,
403 China, *Atmospheric Environment*, 37, 289-298, 10.1016/s1352-2310(02)00832-4, 2003.
- 404 C. Corbin, J., Othman, A., D. Allan, J., R. Worsnop, D., D. Haskins, J., Sierau, B., Lohmann, U., and
405 A. Mensah, A.: Peak-fitting and integration imprecision in the Aerodyne aerosol mass spectrometer:
406 effects of mass accuracy on location-constrained fits, *Atmos. Meas. Tech.*, 8, 4615-4636, 10.5194/amt-
407 8-4615-2015, 2015.
- 408 Carlton, A. G., Wiedinmyer, C., and Kroll, J. H.: A review of Secondary Organic Aerosol (SOA)
409 formation from isoprene, *Atmospheric Chemistry and Physics*, 9, 4987-5005, 2009.
- 410 Caumo, S., Vicente, A., Custodio, D., Alves, C., and Vasconcellos, P.: Organic compounds in
411 particulate and gaseous phase collected in the neighbourhood of an industrial complex in Sao Paulo
412 (Brazil), *Air Quality Atmosphere and Health*, 11, 271-283, 10.1007/s11869-017-0531-7, 2018.
- 413 Chan, A. W. H., Kautzman, K. E., Chhabra, P. S., Surratt, J. D., Chan, M. N., Crouse, J. D., Kuerten,
414 A., Wennberg, P. O., Flagan, R. C., and Seinfeld, J. H.: Secondary organic aerosol formation from
415 photooxidation of naphthalene and alkylnaphthalenes: implications for oxidation of intermediate
416 volatility organic compounds (IVOCs), *Atmospheric Chemistry and Physics*, 9, 3049-3060,
417 10.5194/acp-9-3049-2009, 2009.
- 418 Chan, A. W. H., Isaacman, G., Wilson, K. R., Worton, D. R., Ruehl, C. R., Nah, T., Gentner, D. R.,
419 Dallmann, T. R., Kirchstetter, T. W., Harley, R. A., Gilman, J. B., Kuster, W. C., deGouw, J. A.,
420 Offenberg, J. H., Kleindienst, T. E., Lin, Y. H., Rubitschun, C. L., Surratt, J. D., Hayes, P. L., Jimenez,
421 J. L., and Goldstein, A. H.: Detailed chemical characterization of unresolved complex mixtures in



- 422 atmospheric organics: Insights into emission sources, atmospheric processing, and secondary organic
423 aerosol formation, *Journal of Geophysical Research-Atmospheres*, 118, 6783-6796,
424 10.1002/jgrd.50533, 2013.
- 425 Chowdhury, P. H., He, Q., Male, T. L., Brune, W. H., Rudich, Y., and Pardo, M.: Exposure of Lung
426 Epithelial Cells to Photochemically Aged Secondary Organic Aerosol Shows Increased Toxic Effects,
427 *Environmental Science & Technology Letters*, 5, 424-430, 10.1021/ars.estlett.8b00256, 2018.
- 428 Cubison, M. J., and Jimenez, J. L.: Statistical precision of the intensities retrieved from constrained
429 fitting of overlapping peaks in high-resolution mass spectra, *Atmos. Meas. Tech.*, 8, 2333-2345,
430 10.5194/amt-8-2333-2015, 2015.
- 431 de Gouw, J., and Warneke, C.: Measurements of volatile organic compounds in the earth's atmosphere
432 using proton-transfer-reaction mass spectrometry, *Mass Spectrometry Reviews*, 26, 223-257,
433 10.1002/mas.20119, 2007.
- 434 de Gouw, J. A., Brock, C. A., Atlas, E. L., Bates, T. S., Fehsenfeld, F. C., Goldan, P. D., Holloway, J.
435 S., Kuster, W. C., Lerner, B. M., Matthew, B. M., Middlebrook, A. M., Onasch, T. B., Peltier, R. E.,
436 Quinn, P. K., Senff, C. J., Stohl, A., Sullivan, A. P., Trainer, M., Warneke, C., Weber, R. J., and
437 Williams, E. J.: Sources of particulate matter in the northeastern United States in summer: 1. Direct
438 emissions and secondary formation of organic matter in urban plumes, *Journal of Geophysical*
439 *Research-Atmospheres*, 113, 10.1029/2007jd009243, 2008.
- 440 de Gouw, J. A., Welsh-Bon, D., Warneke, C., Kuster, W. C., Alexander, L., Baker, A. K., Beyersdorf,
441 A. J., Blake, D. R., Canagaratna, M., Celada, A. T., Huey, L. G., Junkermann, W., Onasch, T. B.,
442 Salcido, A., Sjostedt, S. J., Sullivan, A. P., Tanner, D. J., Vargas, O., Weber, R. J., Worsnop, D. R., Yu,
443 X. Y., and Zaveri, R.: Emission and chemistry of organic carbon in the gas and aerosol phase at a sub-
444 urban site near Mexico City in March 2006 during the MILAGRO study, *Atmospheric Chemistry and*
445 *Physics*, 9, 3425-3442, 10.5194/acp-9-3425-2009, 2009.
- 446 de Gouw, J. A., Middlebrook, A. M., Warneke, C., Ahmadov, R., Atlas, E. L., Bahreini, R., Blake, D.
447 R., Brock, C. A., Brioude, J., Fahey, D. W., Fehsenfeld, F. C., Holloway, J. S., Le Henaff, M., Lueb, R.
448 A., McKeen, S. A., Meagher, J. F., Murphy, D. M., Paris, C., Parrish, D. D., Perring, A. E., Pollack, I.
449 B., Ravishankara, A. R., Robinson, A. L., Ryerson, T. B., Schwarz, J. P., Spackman, J. R., Srinivasan,
450 A., and Watts, L. A.: Organic aerosol formation downwind from the Deepwater Horizon oil spill,
451 *Science*, 331, 1295-1299, 10.1126/science.1200320, 2011.
- 452 Donahue, N. M., Robinson, A. L., Stanier, C. O., and Pandis, S. N.: Coupled partitioning, dilution, and
453 chemical aging of semivolatile organics, *Environmental Science & Technology*, 40, 2635-2643,
454 10.1021/es052297c, 2006.
- 455 Dzepina, K., Volkamer, R. M., Madronich, S., Tulet, P., Ulbrich, I. M., Zhang, Q., Cappa, C. D.,
456 Ziemann, P. J., and Jimenez, J. L.: Evaluation of recently-proposed secondary organic aerosol models
457 for a case study in Mexico City, *Atmospheric Chemistry and Physics*, 9, 5681-5709, 10.5194/acp-9-
458 5681-2009, 2009.
- 459 Edney, E. O., Kleindienst, T. E., Jaoui, M., Lewandowski, M., Offenberg, J. H., Wang, W., and Claeys,
460 M.: Formation of 2-methyl tetrols and 2-methylglyceric acid in secondary organic aerosol from
461 laboratory irradiated isoprene/NOX/SO2/air mixtures and their detection in ambient PM2.5 samples
462 collected in the eastern United States, *Atmospheric Environment*, 39, 5281-5289,
463 <https://doi.org/10.1016/j.atmosenv.2005.05.031>, 2005.
- 464 Erickson, M. H., Gueneron, M., and Jobson, T.: Measuring long chain alkanes in diesel engine exhaust
465 by thermal desorption PTR-MS, *Atmospheric Measurement Techniques*, 7, 225-239, 10.5194/amt-7-
466 225-2014, 2014.
- 467 Gentner, D. R., Isaacman, G., Worton, D. R., Chan, A. W. H., Dallmann, T. R., Davis, L., Liu, S., Day,
468 D. A., Russell, L. M., Wilson, K. R., Weber, R., Guha, A., Harley, R. A., and Goldstein, A. H.:
469 Elucidating secondary organic aerosol from diesel and gasoline vehicles through detailed
470 characterization of organic carbon emissions, *Proceedings of the National Academy of Sciences of the*
471 *United States of America*, 109, 18318-18323, 10.1073/pnas.1212272109, 2012.
- 472 Goldstein, A. H., and Galbally, I. E.: Known and Unexplored Organic Constituents in the Earth's
473 Atmosphere, *Environmental Science & Technology*, 41, 1514-1521, 10.1021/es072476p, 2007.
- 474 Gong, P., Wang, X., and Yao, T.: Ambient distribution of particulate- and gas-phase n-alkanes and
475 polycyclic aromatic hydrocarbons in the Tibetan Plateau, *Environmental Earth Sciences*, 64, 1703-1711,
476 10.1007/s12665-011-0974-3, 2011.



- 477 Gueneron, M., Erickson, M. H., VanderSchelden, G. S., and Jobson, B. T.: PTR-MS fragmentation
478 patterns of gasoline hydrocarbons, *International Journal of Mass Spectrometry*, 379, 97-109,
479 10.1016/j.ijms.2015.01.001, 2015.
- 480 Hallquist, M., Wenger, J. C., Baltensperger, U., Rudich, Y., Simpson, D., Claeys, M., Dommen, J.,
481 Donahue, N. M., George, C., Goldstein, A. H., Hamilton, J. F., Herrmann, H., Hoffmann, T., Iinuma,
482 Y., Jang, M., Jenkin, M. E., Jimenez, J. L., Kiendler-Scharr, A., Maenhaut, W., McFiggans, G., Mentel,
483 T. F., Monod, A., Prevot, A. S. H., Seinfeld, J. H., Surratt, J. D., Szmigielski, R., and Wildt, J.: The
484 formation, properties and impact of secondary organic aerosol: current and emerging issues,
485 *Atmospheric Chemistry and Physics*, 9, 5155-5236, 10.5194/acp-9-5155-2009, 2009.
- 486 Hayes, P. L., Carlton, A. G., Baker, K. R., Ahmadov, R., Washenfelder, R. A., Alvarez, S.,
487 Rappenglueck, B., Gilman, J. B., Kuster, W. C., de Gouw, J. A., Zotter, P., Prevot, A. S. H., Szidat, S.,
488 Kleindienst, T. E., Offenberg, J. H., Ma, P. K., and Jimenez, J. L.: Modeling the formation and aging
489 of secondary organic aerosols in Los Angeles during CalNex 2010, *Atmospheric Chemistry and Physics*,
490 15, 5773-5801, 10.5194/acp-15-5773-2015, 2015.
- 491 Hellén, H., Tykkä, T., and Hakola, H.: Importance of monoterpenes and isoprene in urban air in northern
492 Europe, *Atmospheric Environment*, 59, 59-66, <https://doi.org/10.1016/j.atmosenv.2012.04.049>, 2012.
- 493 Hodzic, A., Jimenez, J. L., Madronich, S., Canagaratna, M. R., DeCarlo, P. F., Kleinman, L., and Fast,
494 J.: Modeling organic aerosols in a megacity: potential contribution of semi-volatile and intermediate
495 volatility primary organic compounds to secondary organic aerosol formation, *Atmospheric Chemistry
496 and Physics*, 10, 5491-5514, 10.5194/acp-10-5491-2010, 2010.
- 497 Huang, G., Liu, Y., Shao, M., Li, Y., Chen, Q., Zheng, Y., Wu, Z., Liu, Y., Wu, Y., Hu, M., Li, X., Lu,
498 S., Wang, C., Liu, J., Zheng, M., and Zhu, T.: Potentially Important Contribution of Gas-Phase
499 Oxidation of Naphthalene and Methyl-naphthalene to Secondary Organic Aerosol during Haze Events
500 in Beijing, *Environmental Science & Technology*, 53, 1235-1244, 10.1021/acs.est.8b04523, 2019.
- 501 Inomata, S., Tanimoto, H., and Yamada, H.: Mass Spectrometric Detection of Alkanes Using NO+
502 Chemical Ionization in Proton-transfer-reaction Plus Switchable Reagent Ion Mass Spectrometry,
503 *Chemistry Letters*, 43, 538-540, 10.1246/cl.131105, 2013.
- 504 Isaacman, G., Wilson, K. R., Chan, A. W. H., Worton, D. R., Kimmel, J. R., Nah, T., Hohaus, T., Gonin,
505 M., Kroll, J. H., Worsnop, D. R., and Goldstein, A. H.: Improved Resolution of Hydrocarbon Structures
506 and Constitutional Isomers in Complex Mixtures Using Gas Chromatography-Vacuum Ultraviolet-
507 Mass Spectrometry, *Analytical Chemistry*, 84, 2335-2342, 10.1021/ac2030464, 2012.
- 508 Jathar, S. H., Gordon, T. D., Hennigan, C. J., Pye, H. O. T., Pouliot, G., Adams, P. J., Donahue, N. M.,
509 and Robinson, A. L.: Unspeciated organic emissions from combustion sources and their influence on
510 the secondary organic aerosol budget in the United States, *Proceedings of the National Academy of
511 Sciences of the United States of America*, 111, 10473-10478, 10.1073/pnas.1323740111, 2014.
- 512 Jiang, F., Liu, Q., Huang, X., Wang, T., Zhuang, B., and Xie, M.: Regional modeling of secondary
513 organic aerosol over China using WRF/Chem, *Journal of Aerosol Science*, 43, 57-73,
514 10.1016/j.jaerosci.2011.09.003, 2012.
- 515 Jobson, B. T., Alexander, M. L., Maupin, G. D., and Muntean, G. G.: On-line analysis of organic
516 compounds in diesel exhaust using a proton transfer reaction mass spectrometer (PTR-MS),
517 *International Journal of Mass Spectrometry*, 245, 78-89, 10.1016/j.ijms.2005.05.009, 2005.
- 518 Jordan, A., Haidacher, S., Hanel, G., Hartungen, E., Herbig, J., Maerk, L., Schottkowsky, R., Seehauser,
519 H., Sulzer, P., and Maerk, T. D.: An online ultra-high sensitivity Proton-transfer-reaction mass-
520 spectrometer combined with switchable reagent ion capability (PTR+SRI-MS), *International Journal of
521 Mass Spectrometry*, 286, 32-38, 10.1016/j.ijms.2009.06.006, 2009.
- 522 Keyte, I. J., Harrison, R. M., and Lammel, G.: Chemical reactivity and long-range transport potential
523 of polycyclic aromatic hydrocarbons - a review, *Chemical Society Reviews*, 42, 9333-9391,
524 10.1039/c3cs60147a, 2013.
- 525 Khare, P., and Gentner, D. R.: Considering the future of anthropogenic gas-phase organic compound
526 emissions and the increasing influence of non-combustion sources on urban air quality, *Atmospheric
527 Chemistry and Physics*, 18, 5391-5413, 10.5194/acp-18-5391-2018, 2018.
- 528 Kleindienst, T. E., Edney, E. O., Lewandowski, M., Offenberg, J. H., and Jaoui, M.: Secondary Organic
529 Carbon and Aerosol Yields from the Irradiations of Isoprene and α -Pinene in the Presence of NO_x and
530 SO₂, *Environmental Science & Technology*, 40, 3807-3812, 10.1021/es052446r, 2006.



- 531 Kleindienst, T. E., Jaoui, M., Lewandowski, M., Offenberg, J. H., and Docherty, K. S.: The formation
532 of SOA and chemical tracer compounds from the photooxidation of naphthalene and its methyl analogs
533 in the presence and absence of nitrogen oxides, *Atmospheric Chemistry and Physics*, 12, 8711-8726,
534 10.5194/acp-12-8711-2012, 2012.
- 535 Koss, A. R., Warneke, C., Yuan, B., Coggon, M. M., Veres, P. R., and de Gouw, J. A.: Evaluation of
536 NO⁺ reagent ion chemistry for online measurements of atmospheric volatile organic compounds,
537 *Atmospheric Measurement Techniques*, 9, 2909-2925, 10.5194/amt-9-2909-2016, 2016.
- 538 Lamkaddam, H., Gratién, A., Panguí, E., Cazaunau, M., Picquet-Varrault, B., and Doussin, J.-F.: High-
539 NO_x Photooxidation of n-Dodecane: Temperature Dependence of SOA Formation, *Environmental*
540 *Science & Technology*, 51, 192-201, 10.1021/acs.est.6b03821, 2017a.
- 541 Lamkaddam, H., Gratién, A., Panguí, E., Cazaunau, M., Picquet-Varrault, B., and Doussin, J. F.: High-
542 NO_x Photooxidation of n-Dodecane: Temperature Dependence of SOA Formation, *Environ Sci*
543 *Technol*, 51, 192-201, 10.1021/acs.est.6b03821, 2017b.
- 544 Li, L., Tang, P., Nakao, S., Kacarab, M., and Cocker, D. R., 3rd: Novel Approach for Evaluating
545 Secondary Organic Aerosol from Aromatic Hydrocarbons: Unified Method for Predicting Aerosol
546 Composition and Formation, *Environ Sci Technol*, 50, 6249-6256, 10.1021/acs.est.5b05778, 2016.
- 547 Liang, C., Pankow, J. F., Odum, J. R., and Seinfeld, J. H.: Gas/Particle Partitioning of Semivolatile
548 Organic Compounds To Model Inorganic, Organic, and Ambient Smog Aerosols, *Environmental*
549 *Science & Technology*, 31, 3086-3092, 10.1021/es9702529, 1997.
- 550 Liggio, J., Li, S.-M., Hayden, K., Taha, Y. M., Stroud, C., Darlington, A., Drollette, B. D., Gordon, M.,
551 Lee, P., Liu, P., Leithead, A., Moussa, S. G., Wang, D., O'Brien, J., Mittermeier, R. L., Brook, J. R.,
552 Lu, G., Staebler, R. M., Han, Y., Tokarek, T. W., Osthoff, H. D., Makar, P. A., Zhang, J., L. Plata, D.,
553 and Gentner, D. R.: Oil sands operations as a large source of secondary organic aerosols, *Nature*, 534,
554 91-94, 10.1038/nature17646, 2016.
- 555 Lim, Y. B., and Ziemann, P. J.: Products and mechanism of secondary organic aerosol formation from
556 reactions of n-alkanes with OH radicals in the presence of NO_x, *Environmental Science & Technology*,
557 39, 9229-9236, 10.1021/es051447g, 2005.
- 558 Lim, Y. B., and Ziemann, P. J.: Effects of Molecular Structure on Aerosol Yields from OH Radical-
559 Initiated Reactions of Linear, Branched, and Cyclic Alkanes in the Presence of NO_x, *Environmental*
560 *Science & Technology*, 43, 2328-2334, 10.1021/es803389s, 2009.
- 561 Loza, C. L., Craven, J. S., Yee, L. D., Coggon, M. M., Schwantes, R. H., Shiraiwa, M., Zhang, X.,
562 Schilling, K. A., Ng, N. L., Canagaratna, M. R., Ziemann, P. J., Flagan, R. C., and Seinfeld, J. H.:
563 Secondary organic aerosol yields of 12-carbon alkanes, *Atmospheric Chemistry and Physics*, 14, 1423-
564 1439, 10.5194/acp-14-1423-2014, 2014.
- 565 Ma, P. K., Zhao, Y., Robinson, A. L., Worton, D. R., Goldstein, A. H., Ortega, A. M., Jimenez, J. L.,
566 Zotter, P., Prevot, A. S. H., Szidat, S., and Hayes, P. L.: Evaluating the impact of new observational
567 constraints on P-S/IVOC emissions, multi-generation oxidation, and chamber wall losses on SOA
568 modeling for Los Angeles, CA, *Atmospheric Chemistry and Physics*, 17, 9237-9259, 10.5194/acp-17-
569 9237-2017, 2017.
- 570 McDonald, B. C., de Gouw, J. A., Gilman, J. B., Jathar, S. H., Akherati, A., Cappa, C. D., Jimenez, J.
571 L., Lee-Taylor, J., Hayes, P. L., McKeen, S. A., Cui, Y. Y., Kim, S.-W., Gentner, D. R., Isaacman-
572 VanWertz, G., Goldstein, A. H., Harley, R. A., Frost, G. J., Roberts, J. M., Ryerson, T. B., and Trainer,
573 M.: Volatile chemical products emerging as largest petrochemical source of urban organic emissions,
574 *Science*, 359, 760-764, 10.1126/science.aaq0524, 2018.
- 575 Mikoviny, T., Kaser, L., and Wisthaler, A.: Development and characterization of a High-Temperature
576 Proton-Transfer-Reaction Mass Spectrometer (HT-PTR-MS), *Atmospheric Measurement Techniques*
577 *Discussions*, 3, 185-202, 2010.
- 578 Ng, N. L., Kroll, J. H., Chan, A. W. H., Chhabra, P. S., Flagan, R. C., and Seinfeld, J. H.: Secondary
579 organic aerosol formation from m-xylene, toluene, and benzene, *Atmospheric Chemistry and Physics*,
580 7, 3909-3922, 2007.
- 581 Pandis, S. N., Paulson, S. E., Seinfeld, J. H., and Flagan, R. C.: Aerosol formation in the photooxidation
582 of isoprene and β-pinene, *Atmospheric Environment. Part A. General Topics*, 25, 997-1008,
583 [https://doi.org/10.1016/0960-1686\(91\)90141-S](https://doi.org/10.1016/0960-1686(91)90141-S), 1991.



- 584 Presto, A. A., Miracolo, M. A., Donahue, N. M., and Robinson, A. L.: Secondary Organic Aerosol
585 Formation from High-NO_x Photo-Oxidation of Low Volatility Precursors: n-Alkanes, *Environmental*
586 *Science & Technology*, 44, 2029-2034, 10.1021/es903712r, 2010a.
- 587 Presto, A. A., Miracolo, M. A., Donahue, N. M., and Robinson, A. L.: Secondary organic aerosol
588 formation from high-NO(x) photo-oxidation of low volatility precursors: n-alkanes, *Environ Sci*
589 *Technol*, 44, 2029-2034, 10.1021/es903712r, 2010b.
- 590 Pye, H. O. T., and Pouliot, G. A.: Modeling the Role of Alkanes, Polycyclic Aromatic Hydrocarbons,
591 and Their Oligomers in Secondary Organic Aerosol Formation, *Environmental Science & Technology*,
592 46, 6041-6047, 10.1021/es300409w, 2012.
- 593 Robinson, A. L., Donahue, N. M., Shrivastava, M. K., Weitkamp, E. A., Sage, A. M., Grieshop, A. P.,
594 Lane, T. E., Pierce, J. R., and Pandis, S. N.: Rethinking organic aerosols: Semivolatile emissions and
595 photochemical aging, *Science*, 315, 1259-1262, 10.1126/science.1133061, 2007.
- 596 Sangiorgi, G., Ferrero, L., Perrone, M. G., Papa, E., and Bolzacchini, E.: Semivolatile PAH and n-
597 alkane gas/particle partitioning using the dual model: up-to-date coefficients and comparison with
598 experimental data, *Environmental Science and Pollution Research*, 21, 10163-10173, 10.1007/s11356-
599 014-2902-z, 2014.
- 600 Stark, H., Yatavelli, R. L. N., Thompson, S. L., Kimmel, J. R., Cubison, M. J., Chhabra, P. S.,
601 Canagaratna, M. R., Jayne, J. T., Worsnop, D. R., and Jimenez, J. L.: Methods to extract molecular and
602 bulk chemical information from series of complex mass spectra with limited mass resolution,
603 *International Journal of Mass Spectrometry*, 389, 26-38, <https://doi.org/10.1016/j.ijms.2015.08.011>,
604 2015.
- 605 Tajuelo, M., Rodriguez, D., Teresa Baeza-Romero, M., Diaz-de-Mera, Y., Aranda, A., and Rodriguez,
606 A.: Secondary organic aerosol formation from styrene photolysis and photooxidation with hydroxyl
607 radicals, *Chemosphere*, 231, 276-286, 10.1016/j.chemosphere.2019.05.136, 2019.
- 608 Takekawa, H., Minoura, H., and Yamazaki, S.: Temperature dependence of secondary organic aerosol
609 formation by photo-oxidation of hydrocarbons, *Atmospheric Environment*, 37, 3413-3424,
610 [https://doi.org/10.1016/S1352-2310\(03\)00359-5](https://doi.org/10.1016/S1352-2310(03)00359-5), 2003.
- 611 Timonen, H., Cubison, M., Aurela, M., Brus, D., Lihavainen, H., Hillamo, R., Canagaratna, M., Nekat,
612 B., Weller, R., Worsnop, D., and Saarikoski, S.: Applications and limitations of constrained high-
613 resolution peak fitting on low resolving power mass spectra from the ToF-ACSM, *Atmos. Meas. Tech.*,
614 9, 3263-3281, 10.5194/amt-9-3263-2016, 2016.
- 615 Tkacik, D. S., Presto, A. A., Donahue, N. M., and Robinson, A. L.: Secondary Organic Aerosol
616 Formation from Intermediate-Volatility Organic Compounds: Cyclic, Linear, and Branched Alkanes,
617 *Environmental Science & Technology*, 46, 8773-8781, 10.1021/es301112c, 2012a.
- 618 Tkacik, D. S., Presto, A. A., Donahue, N. M., and Robinson, A. L.: Secondary organic aerosol formation
619 from intermediate-volatility organic compounds: cyclic, linear, and branched alkanes, *Environ Sci*
620 *Technol*, 46, 8773-8781, 10.1021/es301112c, 2012b.
- 621 Wu, L., Wang, X., Lu, S., Shao, M., and Ling, Z.: Emission inventory of semi-volatile and intermediate-
622 volatility organic compounds and their effects on secondary organic aerosol over the Pearl River Delta
623 region, *Atmospheric Chemistry and Physics*, 19, 8141-8161, 10.5194/acp-19-8141-2019, 2019.
- 624 Xie, M., Hannigan, M. P., and Barsanti, K. C.: Gas/particle partitioning of n-alkanes, PAHs and
625 oxygenated PAHs in urban Denver, *Atmospheric Environment*, 95, 355-362,
626 10.1016/j.atmosenv.2014.06.056, 2014.
- 627 Yang, W., Li, J., Wang, M., Sun, Y., and Wang, Z.: A Case Study of Investigating Secondary Organic
628 Aerosol Formation Pathways in Beijing using an Observation-based SOA Box Model, *Aerosol and Air*
629 *Quality Research*, 18, 1606-1616, 10.4209/aaqr.2017.10.0415, 2018.
- 630 Yuan, B., Chen, W. T., Shao, M., Wang, M., Lu, S. H., Wang, B., Liu, Y., Chang, C. C., and Wang, B.
631 G.: Measurements of ambient hydrocarbons and carbonyls in the Pearl River Delta (PRD), China,
632 *Atmospheric Research*, 116, 93-104, 10.1016/j.atmosres.2012.03.006, 2012.
- 633 Yuan, B., Hu, W. W., Shao, M., Wang, M., Chen, W. T., Lu, S. H., Zeng, L. M., and Hu, M.: VOC
634 emissions, evolutions and contributions to SOA formation at a receptor site in eastern China,
635 *Atmospheric Chemistry and Physics*, 13, 8815-8832, 10.5194/acp-13-8815-2013, 2013.
- 636 Yuan, B., Koss, A. R., Warneke, C., Coggon, M., Sekimoto, K., and de Gouw, J. A.: Proton-Transfer-
637 Reaction Mass Spectrometry: Applications in Atmospheric Sciences, *Chem Rev*, 117, 13187-13229,
638 10.1021/acs.chemrev.7b00325, 2017a.



- 639 Yuan, B., Koss, A. R., Warneke, C., Coggon, M., Sekimoto, K., and de Gouw, J. A.: Proton-Transfer-
640 Reaction Mass Spectrometry: Applications in Atmospheric Sciences, *Chemical Reviews*, 117, 13187-
641 13229, 10.1021/acs.chemrev.7b00325, 2017b.
- 642 Zhao, Y., Kreisberg, N. M., Worton, D. R., Teng, A. P., Hering, S. V., and Goldstein, A. H.:
643 Development of an In Situ Thermal Desorption Gas Chromatography Instrument for Quantifying
644 Atmospheric Semi-Volatile Organic Compounds, *Aerosol Science and Technology*, 47, 258-266,
645 10.1080/02786826.2012.747673, 2013.
- 646 Zhao, Y., Hennigan, C. J., May, A. A., Tkacik, D. S., de Gouw, J. A., Gilman, J. B., Kuster, W. C.,
647 Borbon, A., and Robinson, A. L.: Intermediate-Volatility Organic Compounds: A Large Source of
648 Secondary Organic Aerosol, *Environmental Science & Technology*, 48, 13743-13750,
649 10.1021/es5035188, 2014a.
- 650 Zhao, Y., Hennigan, C. J., May, A. A., Tkacik, D. S., de Gouw, J. A., Gilman, J. B., Kuster, W. C.,
651 Borbon, A., and Robinson, A. L.: Intermediate-volatility organic compounds: a large source of
652 secondary organic aerosol, *Environ Sci Technol*, 48, 13743-13750, 10.1021/es5035188, 2014b.
- 653 Zhao, Y., Nguyen, N. T., Presto, A. A., Hennigan, C. J., May, A. A., and Robinson, A. L.: Intermediate
654 Volatility Organic Compound Emissions from On-Road Gasoline Vehicles and Small Off-Road
655 Gasoline Engines, *Environmental Science & Technology*, 50, 4554-4563, 10.1021/acs.est.5b06247,
656 2016a.
- 657 Zhao, Y., Nguyen, N. T., Presto, A. A., Hennigan, C. J., May, A. A., and Robinson, A. L.: Intermediate
658 Volatility Organic Compound Emissions from On-Road Gasoline Vehicles and Small Off-Road
659 Gasoline Engines, *Environ Sci Technol*, 50, 4554-4563, 10.1021/acs.est.5b06247, 2016b.
- 660 Zhu, J., Penner, J. E., Lin, G., Zhou, C., Xu, L., and Zhuang, B.: Mechanism of SOA formation
661 determines magnitude of radiative effects, *Proceedings of the National Academy of Sciences of the*
662 *United States of America*, 114, 12685-12690, 10.1073/pnas.1712273114, 2017.

663



664 **Table 1.** Fractions of product ions (m-1) ions in mass spectra, sensitivities, response time
665 and detection limits of higher alkanes in NO+ PTR-ToF-MS.

Compounds	Ions	Fractions of (m-1) ions (%)	Sensitivities (ncps/ppb)	Response time (s)	Detection limit for 10 s integration (ppt)	Detection limit for 1 min integration (ppt)
<i>n</i> -Octane	C ₈ H ₁₇ ⁺	24	104.6	9.0	3.5	1.3
<i>n</i> -Nonane	C ₉ H ₁₉ ⁺	32	106.3	13.3	3.2	1.2
<i>n</i> - <i>n</i> -Decane	C ₁₀ H ₂₁ ⁺	39	120.9	14.1	3.5	1.3
<i>n</i> -Undecane	C ₁₁ H ₂₃ ⁺	44	140.9	4.2	3.3	1.2
<i>n</i> -Dodecane	C ₁₂ H ₂₅ ⁺	62	156.3	2.0	2.4	0.9
<i>n</i> -Tridecane	C ₁₃ H ₂₇ ⁺	61	186.6	3.4	2.1	0.8
<i>n</i> -Tetradecane	C ₁₄ H ₂₉ ⁺	64	220.7	18.2	1.9	0.7
<i>n</i> -Pentadecane	C ₁₅ H ₃₁ ⁺	84	205.5	7.6	1.7	0.6
<i>n</i> -Hexadecane	C ₁₆ H ₃₃ ⁺	95	/	20.0	1.6	0.6
<i>n</i> -Heptadecane	C ₁₇ H ₃₅ ⁺	82	/	30.7	1.8	0.7
<i>n</i> -Octadecane	C ₁₈ H ₃₇ ⁺	90	/	34.9	1.8	0.7
<i>n</i> -Nonadecane	C ₁₉ H ₃₉ ⁺	71	/	28.8	1.2	0.4
<i>n</i> -Eicosane	C ₂₀ H ₄₁ ⁺	86	/	53.4	1.9	0.7
<i>n</i> -Heneicosane	C ₂₁ H ₄₃ ⁺	/	/	115.9	2.0	0.7

666



667

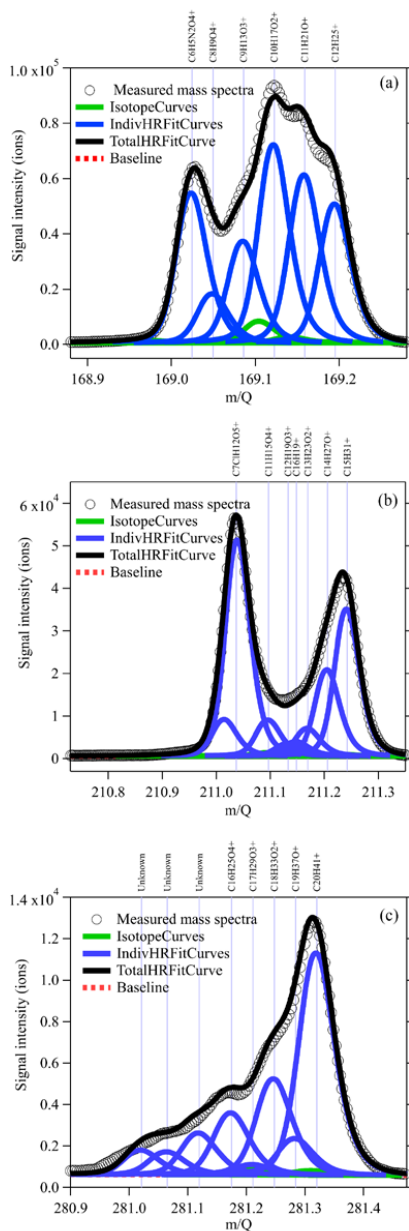
668 **Table 2.** Mean concentrations of alkanes (C8-C21) in different sites worldwide.

Compounds	Formula	PRD, China ^a	PRD, China ^b	NCP, China ^a	Paris, France ^c	Pasadena, US ^d
		Alkanes (ppt)	<i>n</i> -Alkanes (ppt)	Alkanes (ppt)	<i>n</i> -Alkanes (ppt)	Alkanes (ppt)
Octane	C ₈ H ₁₈	482±488	50±49	463±329	/	/
Nonane	C ₉ H ₂₀	208±186	43±32	319±228	14±13	/
Decane	C ₁₀ H ₂₂	174±199	29±28	307±222	24±22	/
Undecane	C ₁₁ H ₂₄	129±138	21±17	239±194	19±16	/
Dodecane	C ₁₂ H ₂₆	122±120	/	156±119	22±21	8±1
Tridecane	C ₁₃ H ₂₈	66±60	/	109±75	13±12	6±1
Tetradecane	C ₁₄ H ₃₀	50±47	/	60±40	27±23	9±2
Pentadecane	C ₁₅ H ₃₂	45±42	/	42±27	23±18	5±0.8
Hexadecane	C ₁₆ H ₃₄	36±33	/	27±17	22±19	4±1
Heptadecane	C ₁₇ H ₃₆	21±20	/	16±11	/	3±0.4
Octadecane	C ₁₈ H ₃₈	13±14	/	10±8	/	1.6±0.5
Nonadecane	C ₁₉ H ₄₀	5±9	/	3±6	/	0.7±0.2
Eicosane	C ₂₀ H ₄₂	0.7±4	/	2±5	/	0.24±0.08
Heneicosane	C ₂₁ H ₄₄	0.5±5	/	2±4	/	0.15±0.1

669 ^a: alkanes measured with NO⁺ PTR-ToF-MS; ^b: *n*-alkanes measured with GC-MS; ^c: *n*-alkanes from Ait-Helal
670 et al. (2014); ^d: *n*-alkanes from Zhao et al. (2014a).

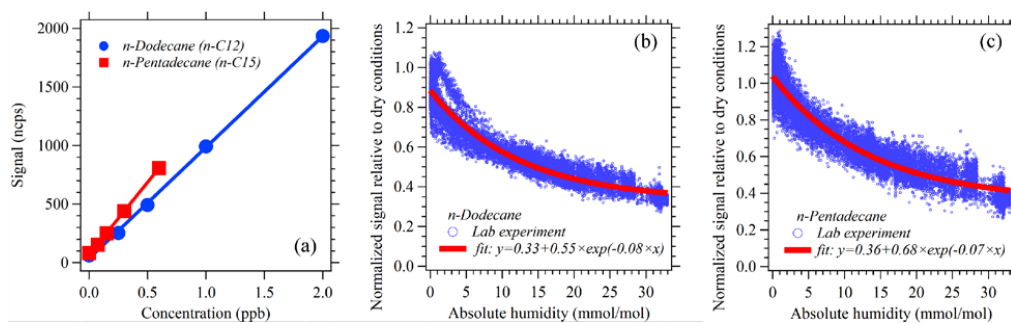
671

672



673

674 **Figure 1.** High-resolution (HR) peak-fitting to the averaged mass spectra on a typical day (12
675 October 2018) for m/z 169 (a), m/z 211 (b) and m/z 281 (c), at which masses produced by
676 dodecane ($C_{12}H_{25}^+$), pentadecane ($C_{15}H_{31}^+$) and eicosane ($C_{20}H_{41}^+$) produced in NO^+ PTR-ToF-
677 MS.

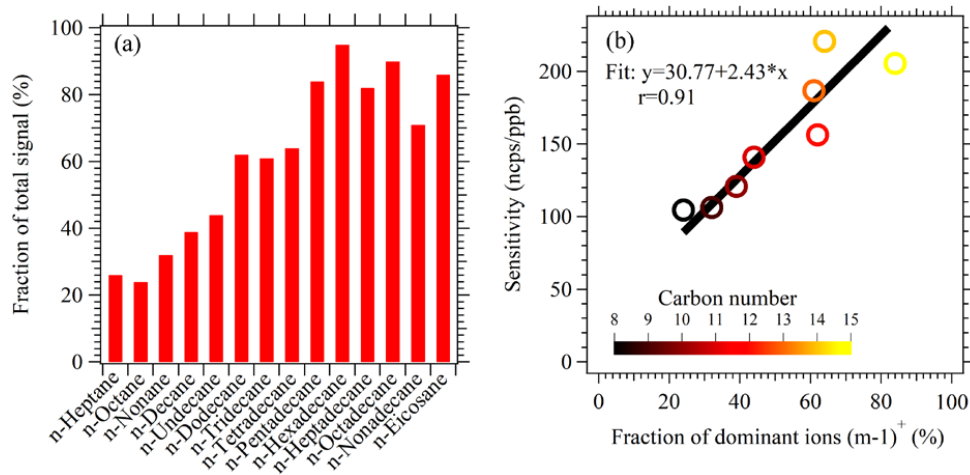


678

679 **Figure 2.** (a) Calibrations of n-Dodecane and n-Pentadecane under dry conditions; (b)

680 Humidity dependence of n-Dodecane. (c) Humidity dependence of n-Pentadecane.

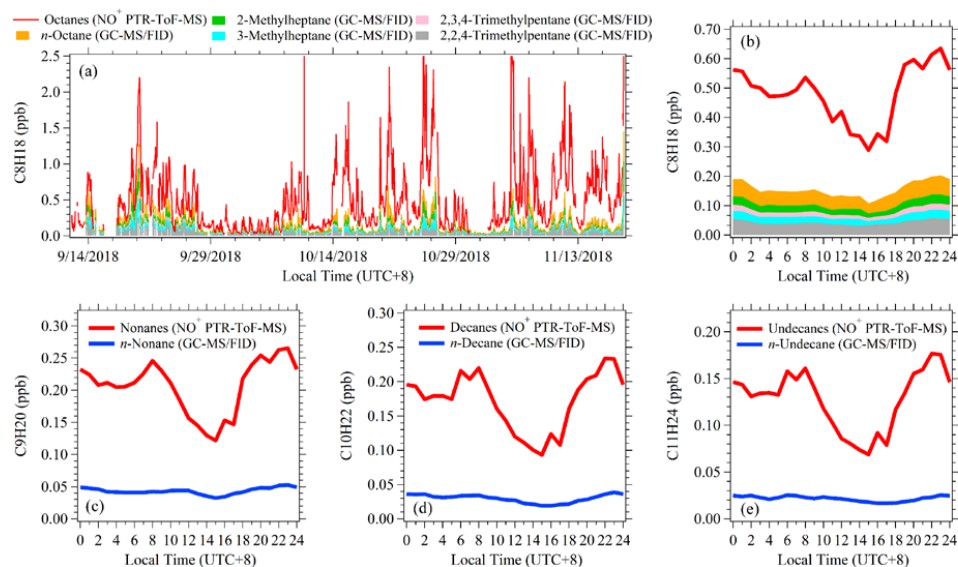
681



682

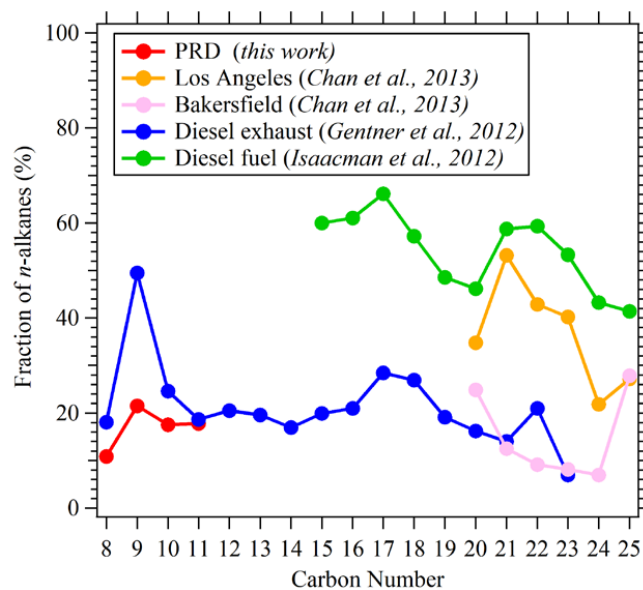
683 **Figure 3.** (a) The fracitons of product ions (m-1) from hydride abstraction of C8-C20 *n*-alkanes
684 in NO⁺ PTR-ToF-MS. (b) Scatterplot of sensitivities under dry conditions versus the fractions
685 of hydride abstraction ions for C8-C15 *n*-alkanes.

686



687

688 **Figure 4.** Comparisons of times series and diurnal variations of alkanes measured by NO⁺
689 PTR-ToF-MS and GC-MS/FID in PRD. (a) Time series of C8 alkanes measured by NO⁺ PTR-
690 ToF-MS, C8 *n*-alkane and four branched isomers measured by GC-MS/FID. (b) Diurnal
691 variations of C8 alkanes. (c-e) Diurnal variations of C9-C11 alkanes with NO⁺ PTR-ToF-MS
692 and C9-C11 *n*-alkanes with GC-MS/FID.

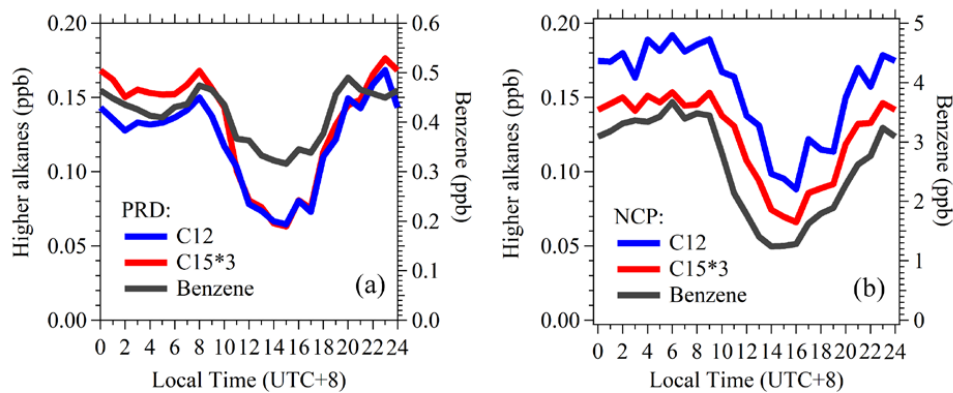


693

694 **Figure 5.** Fractions of *n*-alkanes in higher alkanes derived from this study, ambient air in
695 Los Angeles, Bakersfield and in diesel fuel/exhausts (Chan et al., 2013;Gentner et al.,
696 2012;Isaacman et al., 2012).



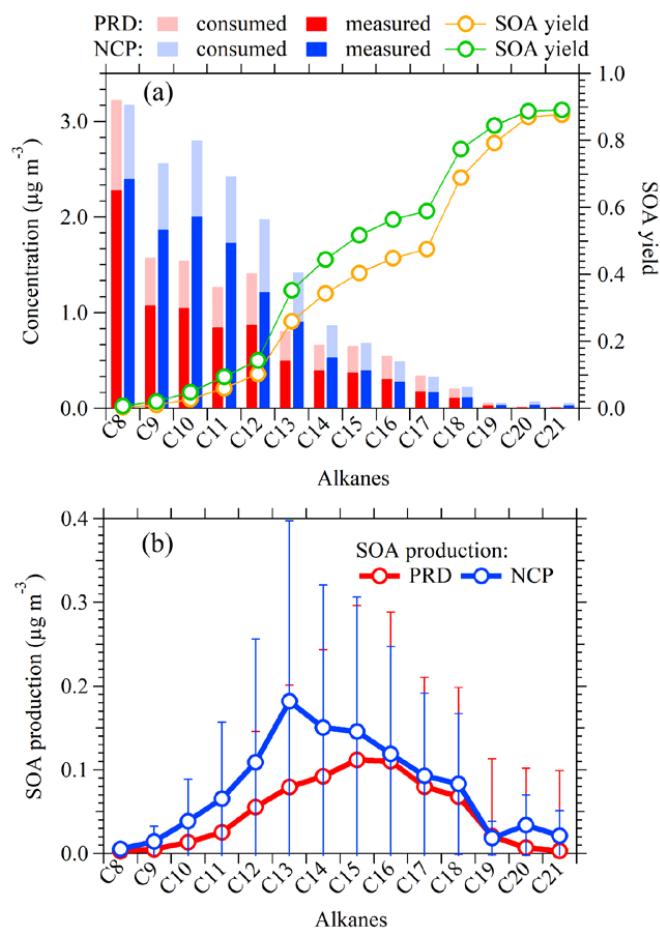
697



698

699 **Figure 6.** Diurnal variations of C12 alkanes, C15 alkanes and benzene in PRD (a) and NCP

700 (b).

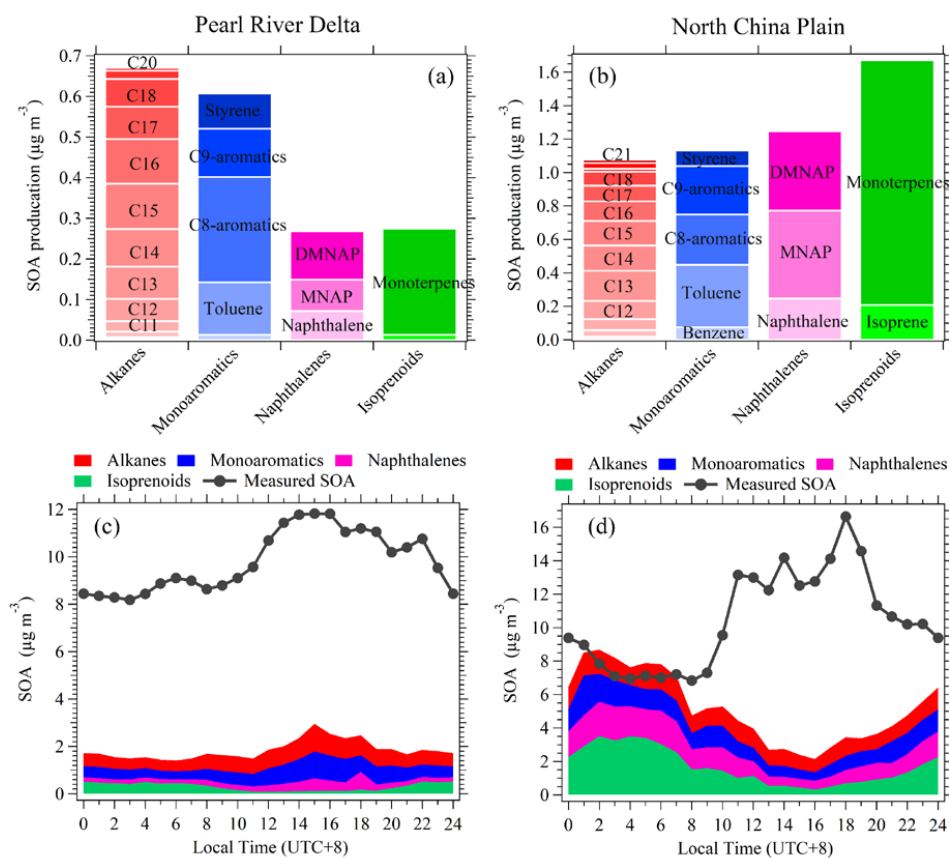


701

702 **Figure 7. (a)** Measured concentrations by NO^+ PTR-ToF-MS, calculated consumed
703 concentrations and average SOA yields for C₈-C₂₁ alkanes in PRD and NCP. **(b)** Calculated
704 average SOA productions for C₈-C₂₁ alkanes in PRD and NCP.



705



706

707 **Figure 8.** The mean concentrations of SOA produced from higher alkanes (C8-C21 alkanes),
 708 monoaromatics (benzene, toluene, C8 aromatics, C9 aromatics and styrene), naphthalenes
 709 (naphthalene, methylnaphthalenes, dimethylnaphthalenes) and isoprenoids (isoprene and
 710 monoterpenes) in PRD (a) and NCP (b). Diurnal variations of SOA production from higher
 711 alkanes, monoaromatics, naphthalenes and isoprenoids as well as the measured SOA
 712 concentrations in PRD (c) and NCP (d).